



## ICANS-XV

15<sup>th</sup> Meeting of the International Collaboration on Advanced Neutron Sources

November 6-9, 2000

Tsukuba, Japan

**23.16****Experimental Study on Mercury Target and Proton Beam Window**

Hidetaka KINOSHITA\*, Masanori KAMINAGA, Katsuhiko HAGA, and Ryutaro HINO

Japan Atomic Energy Research Institute, Tokai-mura, 319-1195, Japan

\*E-mail : kinosita@cat.tokai.jaeri.go.jp

**Abstract**

The design of a MW-class spallation target system using a mercury target is in progress, in order to produce a practical neutron application while keeping to the highest levels of safety. To establish the safety of the spallation target system, it is important to comprehend the thermal-hydraulic properties of mercury. From thermal-hydraulic experiments by using the mercury experimental loop of 20L/min at maximum, the wall friction factor was relatively larger than the Blasius correlation because of effects of wall roughness and the heat transfer coefficients agreed well with the Subbotin correlation. Also for a proton beam window working as a safety barrier between a proton beam line and the target system, high heat removal performance is required to keep structural integrity of the window. Heat transfer experiments were carried out using a rib-roughened narrow rectangular channel under water flowing condition. Heat transfer coefficients obtained by the experiments were about two times higher than those of a smooth channel.

**1. Introduction**

In the Joint Project of High-Intensity Proton Accelerator <sup>(1)</sup>, a next generation neutron source is being developed to utilize high intensity neutrons for using in the fundamental sciences and nuclear engineering fields. Mercury will be used as the target material of MW-class target for JAERI/KEK joint project. A proton beam window, which acts as a boundary between vacuum in the proton beam line and the mercury target system as well as that in a safety hull which will protect mercury spreading in target vessel in case of the target

vessel failure, will be cool down by water flowing through narrow channels. The coolability in the mercury target and beam windows of the proton beam window and the safety hull are important to design the target system in order to keep their structural integrity. But heat transfer coefficient and pressure loss characteristics with mercury flow or heat transfer coefficient and CHF with water in narrow channel with micro-ribs are not well known. In previous research, heat transfer coefficients of liquid metal including mercury were experimentally measured, but detail conditions of these experiments are not clear today. Also experiments of heat transfer coefficients, the CHF and the friction factor with water in micro-rib roughened narrow rectangular channel are very scarce. Therefore we planned to clarify the heat transfer coefficients of mercury in circular tube and water in micro-rib roughened narrow rectangular channel, in order to develop the mercury target system.

This paper presents experimental results on the heat transfer obtained by using mercury experimental loop and a water loop with micro-rib roughened narrow rectangular channel

## 2. Heat Transfer Experiments with Mercury

### 2.1 Schematics of Mercury Experimental Loop

Figure 2.1 shows the mercury experimental loop of JAERI. The loop consists of a heated test section, an expansion pot, an electro-magnetic pump, a gear pump, an electro-magnetic flow meter and a heat exchanger. Piping size is 25A-Sch80 (inner diameter is 25mm). Figure 2.2 shows a schematic drawing of the mercury loop. Heated test section is circular tube of 15A-Sch80 (inner diameter is 14.3mm) and 1000 mm length (heated length is 600mm). The expansion pot is pressurized by argon gas to keep constant pressure in the loop. Two pumps are installed in parallel to use independently. Elevation change is about 1.5m and total piping length of the loop is about 11m. Inventory of mercury is about 30 little at maximum. All components are made

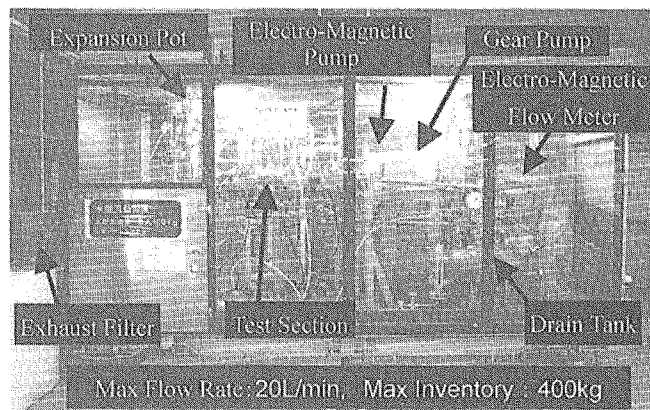


Fig. 2.1 Outer View of the Mercury Experimental Loop.

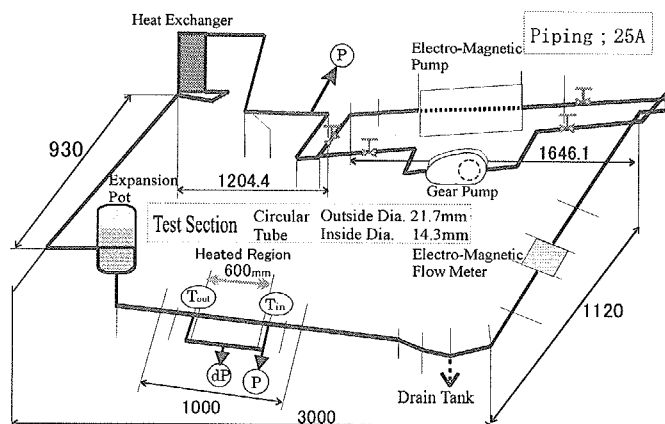


Fig. 2.2 Schematic of the Mercury Experimental Loop.

of SUS316 stainless. To protect the leakage of mercury and its vapor, acryl plates cover this loop, and charcoal filter is installed in an exhaust system.

Specifications of the mercury experimental loop are as follows;

#### Flow Rate

: 15 little/min ( $2.5 \times 10^{-4} \text{ m}^3/\text{s}$ )

by Electro-Magnetic Pump

20 little/min ( $3.3 \times 10^{-4} \text{ m}^3/\text{s}$ )

by Gear Pump

Inventory : Max 30 little

At testing 20 little

Material : SUS316

Pressure : Max

0.5MPa

At testing

0.4MPa

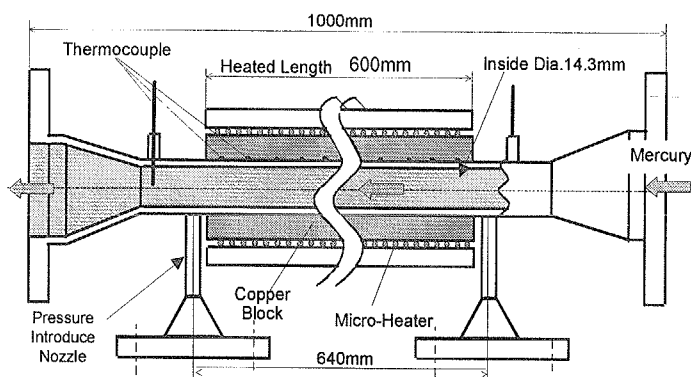


Fig. 2.3 Schematic drawing of the Test Section.

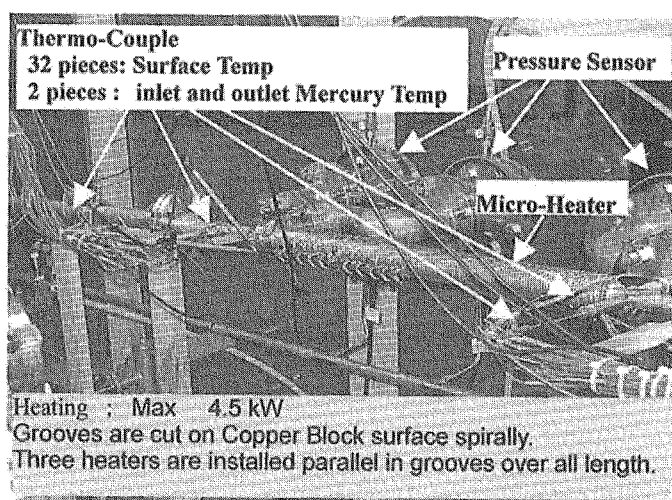


Figure 2.4 outer View of the Test Section.

Figure 2.3 shows a schematic drawing of the heated test section, and figure 2.4 shows outer view. The test section is a stainless steel tube covered with heater block of 4.5 kW. 32 thermocouples are installed on the stainless steel tube surface. Two thermocouples are inserted into the tube to measure inlet and outlet mercury temperature. Pressure loss was also measured in the distance of 640mm including the heated region.

## 2.2 Experimental Condition

The experimental conditions are as follows.

Flow Rate : 0 ~ 10 little/min (Electro-Magnetic Pump)

8.5 ~ 20 little/min (Gear Pump)

Velocity : ~ 2 m/s

Pressure : 0.4MPa

Inlet Temperature : ~40°C

Surface temperature inside of the stainless steel tube is calculated by using one dimensional heat conduction equation under a steady-state condition. Mercury temperature at the test section inlet was several degrees higher when the using electro-magnetic pump, since the mercury was heated by a magnet coil.

### 2.3 Experimental Results

Figure 2.5 shows the relationship between friction factor and Reynolds number. The Blasius correlation is also shown in Fig.2.5. In the case of about 1.0m/s of the mercury velocity, the pressure drop reaches about 9000 Pa, which is about 80% higher than that estimated by the Blasius correlation. In turbulent flow region as shown in the figure, experimental data are about 50 ~ 80 % higher than the Blasius correlation. This would be caused by relatively large wall roughness. However, friction factors obtained by a machined test section agreed well with the Blasius correlation<sup>(2)</sup>, which carried out during commissioning test of the loop.

Figure 2.6 shows the relationship between the Nusselt number and Peclet number. The Peclet number is product of the Reynolds number and the Prandtl number ( $Pe=Re \times Pr$ ). In this figure, the previous experimental results and following correlations<sup>(4)</sup> are also shown.

Martinelli-Lyon correlation (1949)

$$Nu = 7 + 0.025Pe^{0.8} \quad (1)$$

Subbotin Correlation (1962)

$$Nu = 5 + 0.025Pe^{0.8} \quad (2)$$

Lubarsky and Kaufman correlation (1955)

$$Nu = 0.625Pe^{0.4} \quad (3)$$

SNS Design correlation by Siman-Tov et al. <sup>(3)</sup>(1997)

$$Nu = 0.685Pe^{0.372612} \quad (4)$$

Our experimental results agreed well with the Subbotin, and were expressed as follows.

$$Nu = 0.5603Pe^{0.4475} \quad (5)$$

For example, the heat transfer coefficient is about 3500 W/m<sup>2</sup>·K obtained under the the lowest mercury velocity (about 0.05m/sec). And the heat transfer coefficient about 18000 W/m<sup>2</sup>·K under the condition of the mercury velocity of 2.0m/s.

We will accumulate more experimental data to improve above correlations.

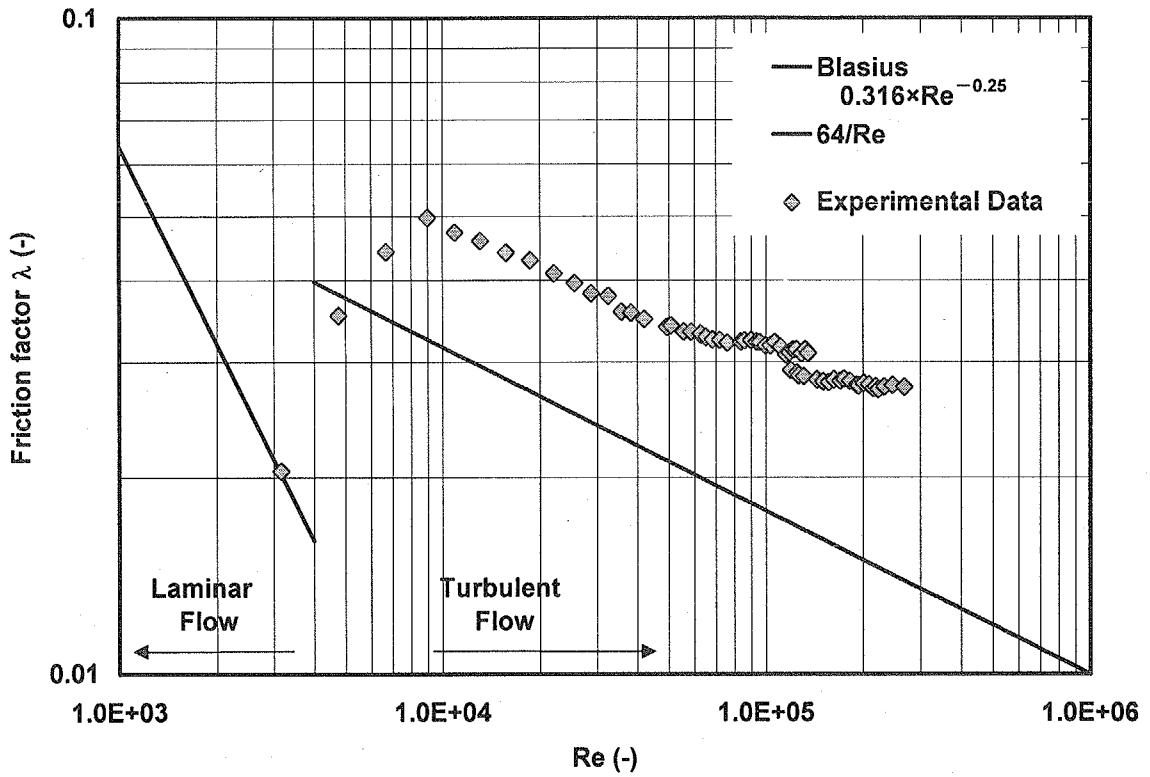


Figure 2.5 Relationship between Friction factor and Reynolds number.

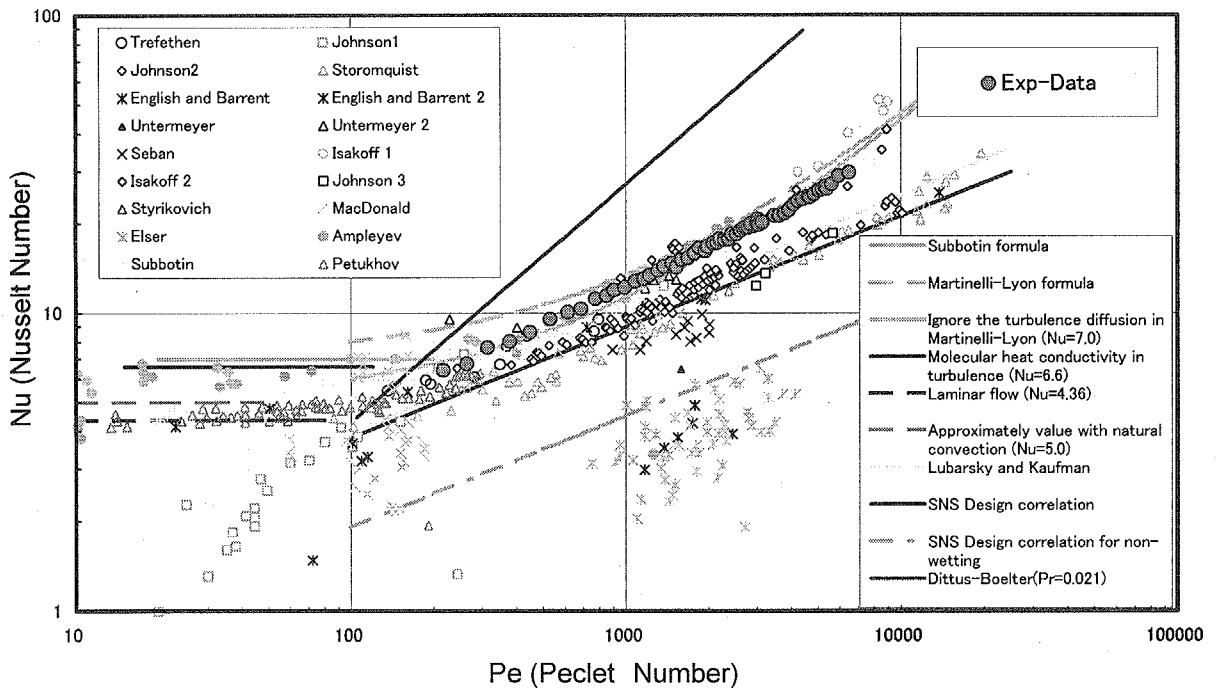


Figure 2.6 Relationship between Nusselt number and Peclet number with Previous Experimental Data and Correlations.

### 3. Heat Transfer Experiments with Water in Rib-Roughened Narrow Rectangular Channel

#### 3.1 Experimental Facility

Figure 3.1 shows a schematic diagram of the CHF test loop. The test loop is composed of a heat exchanger, a re-circulation line, pumps, a mass flow meter and a test section with the narrow rectangular channel in it. Water is used as the coolant in these experiments. The heat exchanger installed in the loop has a heat removal capacity up to 180 kW and about 0.1 m<sup>3</sup> in volume for primary coolant. During experiments, the inlet temperature of coolant will be kept by using the heat exchanger and the inlet pressure will be kept by using a surge tank. Pressure is controlled by pressurized N<sub>2</sub> gas. Either upward or downward flow can be selected by using stop valves.

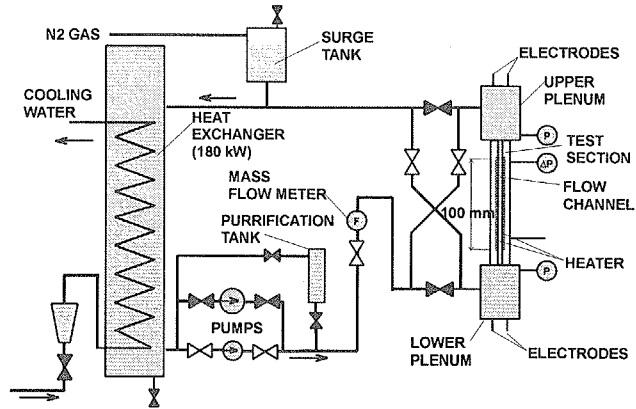


Figure 3.1 Schematic diagram of CHF test loop.

The test section has lower and upper plenums as shown in Fig.3.2. Figure 3.3 shows a schematic of test section. The configuration of the rectangular flow channel is 1.2 mm in water gap, 18 mm in width and 204 mm in length. The coolant is heated from both sides by a heater with a smooth surface and a heater with micro-ribs with rib-pitch ( $p$ ) to rib-height ( $k$ ) ratio  $p/k$

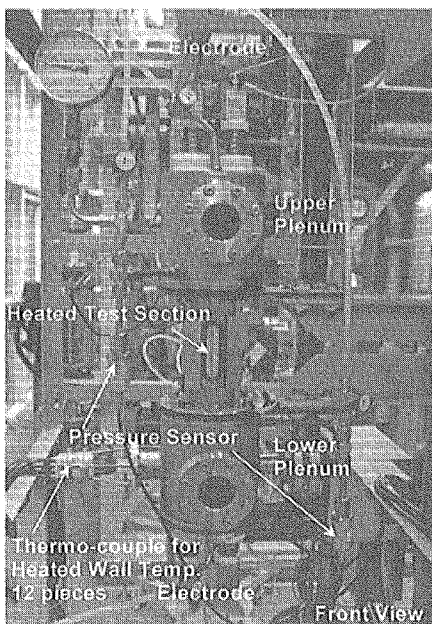


Figure 3.2 Outer view of CHF test section.

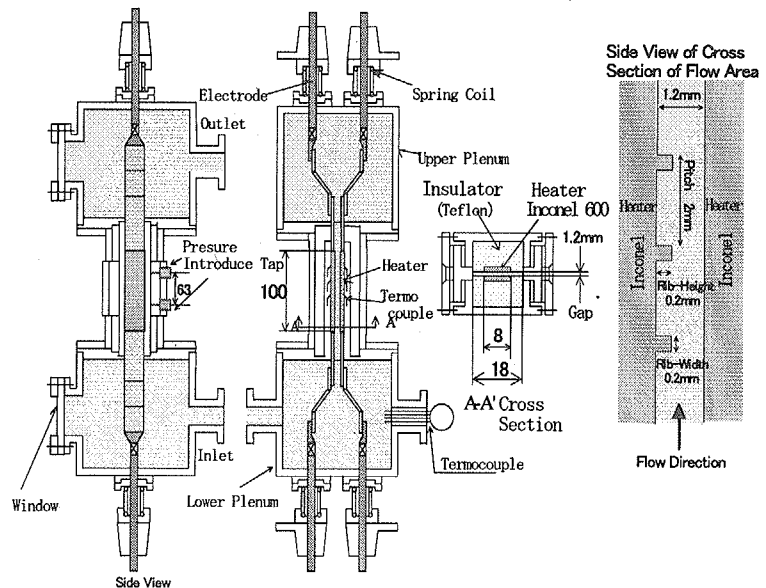


Figure 3.3 Schematic drawing of the CHF test section.

=10. One side heating by each of heaters can also be selected. The dimensions of micro-ribs are 0.2 mm in rib-height ( $k$ ), 0.2 mm in rib-width and 2.0 mm in rib-pitch ( $p$ ). The dimensions of the heaters are 8 mm in width and 100 mm in length. Both heaters are made of Inconel 600 and heated by a direct current up to  $24 \text{ MW/m}^2$  by using a DC power supply. A test section without micro-ribs will also be used to understand the effect of micro-ribs on CHF.

Major parameters in this experiments are heat input, flow rate of water, inlet coolant temperature, the presence/absence of micro-ribs and one/both side(s) heating. The experiment will cover a velocity range of 0.1 to 6 m/s for upward flow.

Specifications of these facilities are as follows.

|                 |   |
|-----------------|---|
| DC Power source | : $\sim 42 \text{ kW}$ ( $20\text{V} \times 2100\text{A}$ ) |
| Flow Rate       | : $\sim 12.0 \text{ kg/sec}$                                |
| Heater Material | : Inconel 600   |
| Heated Length   | : 100mm   |
| Pressure        | : $\sim 0.5 \text{ MPa}$ (abs.)                             |

### 3.2 Experimental Condition

The Experimental conditions are as follows.

|                              |  |
|------------------------------|--|
| Heater Power                 | : 21 kW (each side heating)                                  |
| Heat flux                    | : $\sim 3.6 \text{ MW/m}^2$ (Maximum ; $24 \text{ MW/m}^2$ ) |
| Velocity at test section     | : 1.4 $\sim$ 6.0m/s  |
| Test section outlet pressure | : about 0.4 MPa  |
| Inlet temperature            | : about $25^\circ\text{C}$                                   |

### 3.3 Experimental Results of Friction Factor, Heat Transfer Coefficient and CHF

Single phase forced convection heat transfer coefficients and friction factors were measured before CHF experiments to verify the test section design by comparing with existing experimental results obtained for channels with micro-ribs. During heat transfer experiments, the coolant was heated from the heater with micro-ribs (one side heating) and the coolant velocity was changed from 1.4 to 6.0 m/s ( $Re = 3500$  to  $14600$ ), while the inlet coolant temperature was kept almost constant of  $25.0$  to  $25.8^\circ\text{C}$ .

Figure 3.4 shows friction factors measured in this study for  $Re$  larger than 3000. The solid bold line through the data points is the least-square fit shown as follows.

$$f = 0.110 \cdot Re^{-0.16} \quad (6)$$

In Fig.3.4, the following correlation obtained for a micro-ribbed channel with  $p/k = 10$  by Takase and Hino<sup>(5)</sup> and the Blasius correlation for smooth surfaces are also shown.

$$f = 0.1222 \cdot Re^{-0.147} \quad (7)$$

Measured friction factors are about 186 to 234% higher than the friction factors estimated by the Blasius correlation and -19 to -21 % lower than those estimated by Eq.(7). As shown in Fig.3.4, present results show good agreement with the existing correlation of Eq.(7) allowing the error of about 20%.

Figure 3.5 shows the relationship between Nusselt number and Reynolds number for upward flow under single-phase forced convection where  $Re$  larger than 3500 obtained in this study. Heat losses from the test section were evaluated to be less than 5% during the experiments. Experimental results can be correlated well by the following correlation.

$$Nu = 0.0755 \cdot Re^{0.740} \cdot Pr^{0.4} \quad (8)$$

In Fig.3.5, the following heat transfer correlation obtained for a micro-ribbed channel with  $p/k=10$  by Takase and Hino<sup>(5)</sup> and the Dittus-Boelter correlation are also shown.

$$Nu = 0.0844 \cdot Re^{0.738} \cdot Pr^{0.4} \quad (9)$$

Heat transfer coefficients obtained in this study are 63 to 148% (on the average 92%) higher than those estimated by the Dittus-Boelter correlation and -21 to 18 % (on the average -8%) lower/higher than those estimated by Eq.(9). As shown in Fig.3.5, Eq.(9) gives good prediction within the error of -21 to 18%.

From the above results, it can be concluded that the heat transfer and friction loss characteristics obtained for the test section used in this study were consistent with the existing experimental results.

Figure 3.6 shows the CHF experimental result, and CHF predicted by Sudo correlation<sup>(6)</sup> and CHF predicted by Sudo model<sup>(7)</sup> for the test section investigated in this study heated from one side. During the CHF experiment, the coolant was heated from the heater with micro-ribs and the heat flux of the heater increased step-wisely until any of thermocouples attached on the back surface of the heater detects the CHF. Only one thermocouple located near the exit ( $L_h=90\text{mm}$ ) was connected to the CHF detection system, which can shut off the DC power supply. In the experiment, CHF was occurred at the location of  $L_h=75\text{ mm}$ , therefore when the CHF detection system detected CHF, it was too late to prevent the burnout of the heater as shown in Fig.3.7. CHF was occurred under following conditions.

$$v=1.38\text{ m/s}, \Delta T_{SUB,in}=77.5\text{ }^\circ\text{C}, \Delta T_{SUB,o}=49.1\text{ }^\circ\text{C} \text{ and } q_{CHF}=3.58\text{ MW/m}^2.$$

The CHF predicted by Sudo correlation and Sudo model increase with an increase of coolant velocity for both cases. Sudo correlation gives higher CHF than Sudo model in this case. CHF data obtained in this study agreed well with Sudo model, even the model was obtained for a channel without micro-ribs. At present, only one data was obtained and it is difficult to conclude the CHF for the channels with micro-ribs. More CHF data will have to be accumulated to understand the CHF.



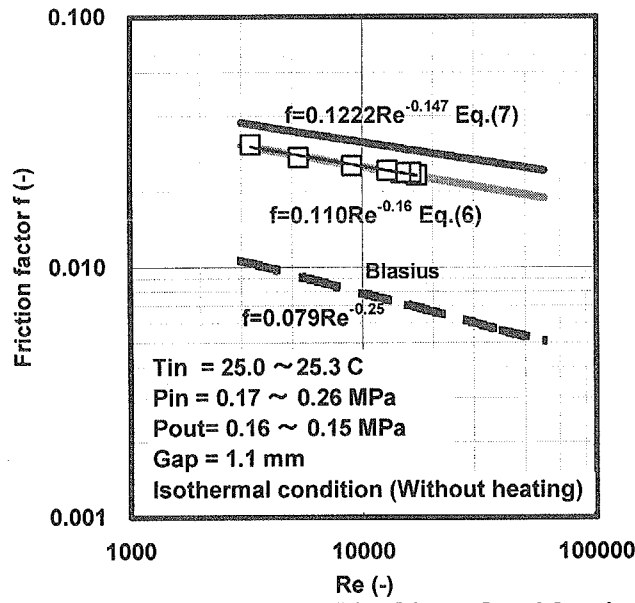


Figure 3.4 Friction factors measured in this study with existing correlations.

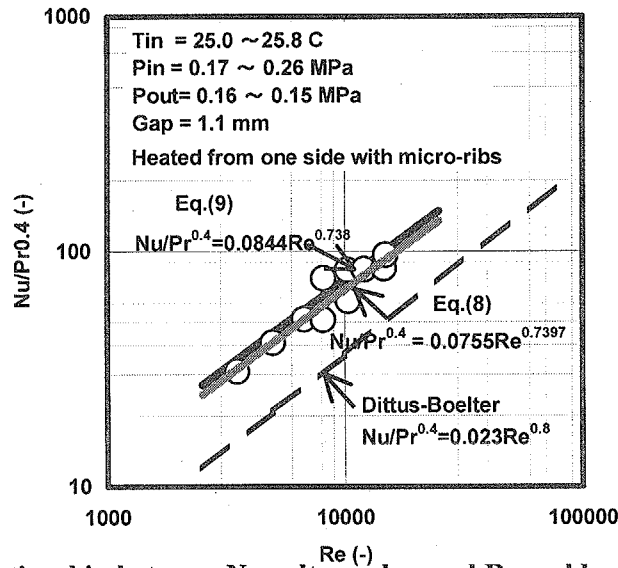


Figure 3.5 Relationship between Nusselt number and Reynolds number in this study.

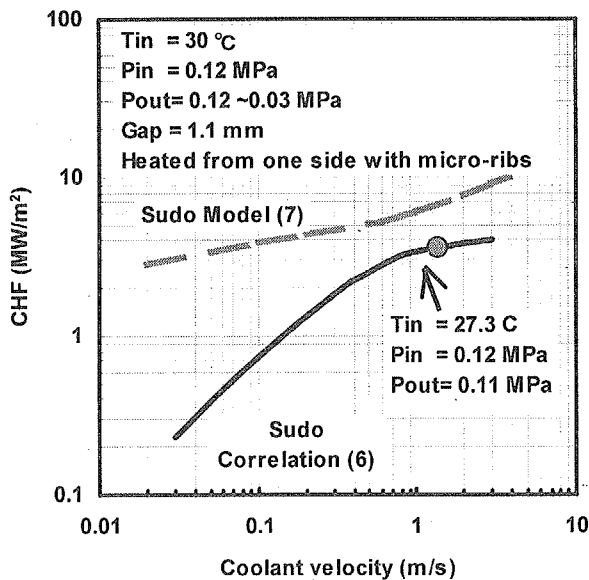


Figure 3.6 Comparisons between CHF data and prediction by Sudo correlation and Sudo model.

#### 4. Concluding Remarks

Thermal Hydraulic experiments with mercury and Heat transfer experiments with water in rib-roughened narrow rectangular channel are conducted, and conclusion obtained by these experiments are as follows;

1. Pressure drop is much larger than the Blasius correlation because wall roughness is relatively large.
2. Heat transfer coefficients agreed well with the Subbotin correlation. And the data are expressed as follows.

$$Nu = 0.5603Pe^{0.4475}$$

3. Friction factor with water in rib-roughened narrow rectangular channel is about 200% higher than those by the Blasius Correlation.
4. Heat transfer coefficients with water in rib-roughened narrow rectangular channel is about two times as those by the Dittus-Boelter Correlation.
5. Only one CHF data was obtained and it is difficult to conclude the CHF for the channels with micro-ribs. Then more CHF data will have to be accumulated to know the CHF characteristics in tube with micro-rib.

Based on these results, we will conduct much more experiments and use the experimental data for detail analyses and design of mercury target and proton beam window

#### References

- (1) The Joint Project Team of JAERI and KEK, "The Joint Project for High-Intensity Proton Accelerators", JAERI-Tech 99-056, (1999-8)
- (2) Kaminaga M., Terada A., Ishikura S., Teshigawara M., Sudo Y. and Hino R., "Mercury Target Development for JAERI Spallation Neutron Source", Proc of ICONE 7, ICONE-7123, (1999-4)
- (3) Siman-Tov M., Wendel M., Haines J. and Rogers M., "Thermal-Hydraulic Analysis of the Liquid Mercury Target for the National Spallation Neutron Source" Proc of Reactor Safety(ARS'97), Orlando, Florida, (1997-6)
- (4) JSME, "JSME Data Book : Heat Transfer -4<sup>th</sup> Edition-" p107,(1997) (in Japanese)
- (5) Takase, K., Hino, R. and Miyamoto Y., "Thermal and Hydraulic Performances of Fuel Rods with Transverse Square Ribs in HTTR", J. Atomic Energy Society of Japan 35(11), (1993), pp 996-998.
- (6) Sudo, Y. and Kaminaga, M., "A New CHF Correlation Scheme Proposed for Vertical Rectangular Channels Heated from Both Sides in Nuclear Research Reactors", Trans. ASME., J. of Heat Transfer, 115 (1993), pp 426-434
- (7) Sudo, Y. and Kaminaga, M., "Critical Heat Flux at High Velocity Channel with High subcooling", Nucl. Eng. and Design 187, (1999), pp215-227.